Performance of acid-activated water caltrop (*Trapa natans*) shell in fixed bed column for hexavalent chromium removal from simulated wastewater

Shravan Kumar[1] · Chandi Patra[2] · Selvaraju Narayanasamy[2] · Prasanna Venkatesh Rajaraman[1]

Abstract

The current study deals with the adsorption of hexavalent chromium using acid (H_3PO_4)-activated water caltrop (*Trapa natans*) shell (PWCS) using an up-flow packed bed column. Characteristics of breakthrough curve was obtained by investigating the effect of several operating parameters viz. inlet flow rate (2–6 mL/min), initial metal ion concentration (50–150 mg/L), and adsorbent's column bed height (1–3 cm). Elevated time of breakthrough curve was reported with elevated adsorbent bed height and vice versa with enhanced initial metal concentration and inlet flow rate of sorbate solution. Process design and breakthrough curves under varying conditions were predicted by applying column models like Thomas model, Adams–Bohart model, Yoon Nelson model, and bed depth service Time (BDST). Column behavior was better described by the BDST and Thomas model and simultaneously gave a good fit with the experimental data of breakthrough curves. The percentage removal for Cr(VI) from aqueous solution having pH 2 and temperature 303.15 K was observed to be 52.46%. The maximum adsorption capacity was found to be 87.31 mg/g according to the Thomas model. Conclusively, phosphoric acid–modified *T. natans* shell (PWCS) showed better sorption potential for of Cr(VI) species from simulated wastewater.

Keywords Acid-activated water caltrop (*Trapa natans*) shell · Hexavalent chromium · Adsorption · Fixed bed column · Column modeling

Introduction

Discharging untreated wastewater containing heavy metals has increased over the past few years due to constant anthropogenic activities, in order to meet the requirement of a rapidly growing population. Water contaminated with heavy metal has been a serious problem of concern around the world (Kelly-Vargas et al. 2012). Heavy metals are the important pollutant in wastewater and their toxicity is a significant issue, which is threatening the environment and imposing serious health problem to humans and other living forms (Rai et al. 2019). Several toxic regularity authorities reported chromium among the top 20 heavy metal list which are deleterious in several aspects like its non-biodegradable and persistent nature (Rai et al. 2019). Chromium (Cr) is considered among the most severely intoxicated heavy metal which is discharged in wastewater through various industries like electroplating, alloy manufacturing, cement, petroleum refining, wood preservation, leather, textiles, etc. (Yu et al. 2018; Almeida et al. 2019; Ma et al. 2019; Cherdchoo et al. 2019). In general, chromium exists in various hexavalent and trivalent oxidation forms among which the hexavalent form deems to be hazardous for humans and other living forms of the ecosystem (El-Sherif et al. 2013). Trivalent chromium (Cr(III)), however, is among the essential micronutrients required for human, animal, and plant metabolism (Cherdchoo et al. 2019).Toxic properties of Cr(VI) can be due to its various factors viz. its oxidative potential, permeability across the cell membrane, and its mobility and solubility (El-Sherif et al. 2013). USEPA defined the maximum tolerable limit for Cr(VI) species in surface

✉ Prasanna Venkatesh Rajaraman
rprasanna@iitg.ac.in

[1] Department of Chemical Engineering, Indian Institute of Technology, Guwahati, Assam 781039, India

[2] Department of Biosciences and Bioengineering, Indian Institute of Technology, Guwahati, Assam 781039, India

water and in wastewater as 0.05 mg/L and 0.5 mg/L, respectively (EPA 1990; Lyu et al. 2017). Moreover, according to WHO, the maximum controlled limit of total chromium (Cr(VI) and Cr(III) species) and other forms of chromium is 2 mg/L (WHO 2004). Hexavalent forms of chromium are responsible for various health issues like digestive tract and lung tumors, skin irritation, ulcer, diarrhea, vomiting, and kidney damage (Rai et al. 2016; Owalude and Tella 2016; Kan et al. 2017). Therefore, it is required to regulate the release of chromium containing effluent in environment through the mechanism of standard law of regulatory authority. Numerous researchers have shown their effort for the remediation of chromium from wastewater via several conventional technologies like membrane filtration, precipitation, coagulation/flocculation, ion exchange, electro-chemical treatment, and reverse osmosis (Almeida et al. 2019; Owalude and Tella 2016). However, most of these conventional methods have significant drawbacks including low efficiency, high energy consumption, more reagent requirement, high cost, and generation of more wastewater and toxic sludge (Patra et al. 2019). Due to such limitations, adsorption can be considered as a promising technique owing to its cheaper, more efficient, and ease-of-operation properties (Zhang et al. 2018). Since past few decades, several adsorbents viz. mineral based, industrial by-product, zeolite, organic, polymeric material, biomass, and agriculture waste have been used in wastewater treatment (Barakat 2011). Recently, various investigations have been carried out on agriculture waste–based feedstock as an alternative for cheap and economically scalable adsorbent for potent remediation of Cr(VI) species from wastewater (Owalude and Tella 2016). Until now, agriculture waste–based activated carbon has been employed for remediation of Cr(VI) from wastewater viz. apricot stone (Demirbas et al. 2004), coconut shell (Pillai et al. 2014), groundnut husk (Dubey and Gopal 2007), activated carbon from rice husk (Bishnoi et al. 2004), *Terminalia arjuna* nuts (Mohanty et al. 2005), etc. However, no research has been reported on the potential of acid-activated *Trapa natans* shell in remediation of chromium from wastewater in fixed bed column. In our previous study, adsorption capacity of raw *T. natans* shell adsorbent was investigated in batch mode for sequestering Cr(VI) species from synthetic water. Therefore, the current study demonstrated the potential of H_3PO_4 acid-activated carbon prepared from *T. natans* shell for removal of Cr(VI) species from synthetic water in continuous fixed bed column. Effect of several adsorption functions in continuous column like adsorbent's column bed depth, initial metal ion concentration, and adsorbate flow rates were investigated. Moreover, Thomas, Adams–Bohart, Yoon–Nelson, and bed depth service time (BDST) model were studied to define the characteristics of breakthrough curve.

Materials and methods

Synthesis of acid-modified *T. natans* shell adsorbent

The *T. natans* shells were collected form Guwahati, Assam, India. The collected sample was thoroughly washed with distilled water and then oven dried at 333 K for 48 h. Further, the dried WC shell was crushed to powdered form and then it was sieved to different sizes for further use. The powder was then treated with 88% H_3PO_4 by following the procedure reported by Rangabhashiyam et al. (2016). Biomass and acid were mixed in the ratio of 1:25 (weight of biomass/volume of chemical) following which the mixture was oven dried at 380 K for 2–3 h. Further, the dried mixture was pyrolyzed in a furnace at 673 K for 1.5 h. To clear away the remnant acid from the resulted mixture, it was rinsed with sodium bicarbonate solution followed by distilled water until the pH of carbonized sample's filtrate was neutral. Thereafter, it was oven dried at 378 K for 24 h and then the carbonized sample referred as ortho-phosphoric acid–modified *T. natans* shell (PWCS) was stored for further use. Further, the specific surface area of the prepared adsorbent was carried out by BET total pore analysis using Micromeritics Instrument (Tristar II; M/s Micromeritics, Norcross, GA, USA). Surface elemental (C, H, N, S) proportion analysis was estimated using CHNS analyzer (Eurovector EA3000).

Synthesis of adsorbate/Cr(VI) solution

All chemicals required for the current study were purchased from HiMedia Pvt. Ltd. Aqueous stock solution (1000 mg/L) for Cr(VI) species was prepared by adding 2.8287 g $K_2Cr_2O_7$ in 1 L distilled water. Working solutions in the range from 50 to 150 mg/L was prepared using the stock and the pH of the same was set utilizing 0.1 M HCl and 0.1 M NaOH.

The packed bed column experiments were studied in a Perspex glass column with an inner diameter of 2 cm and column height of 15 cm (shown in Fig. 1). In a typical experiment, desired quantities of PWCS placed in the glass column for a desired bed height in between glass wool layers were obtained. Thereafter, uniform flow rate of metal solution was obtained by placing glass beads on top as well as on the bottom of the glass wool in the column. Continuous adsorption investigations were performed using peristaltic pump (Miclins, India) under optimized conditions such as pH 2.0 of solution and temperature 303 K for the removal of Cr(VI) ion. The optimization studies have been reported in our previous batch adsorption studies (Kumar et al. 2018). The experiment was carried out by pumping a known metal concentration of solution at pH 2.0 in column using a peristaltic pump (Miclins, India). Cr(VI) sorbate solution was pumped upwards through the adsorbent bed at fixed flow rates and at room temperature. A series of studies were conducted to investigate
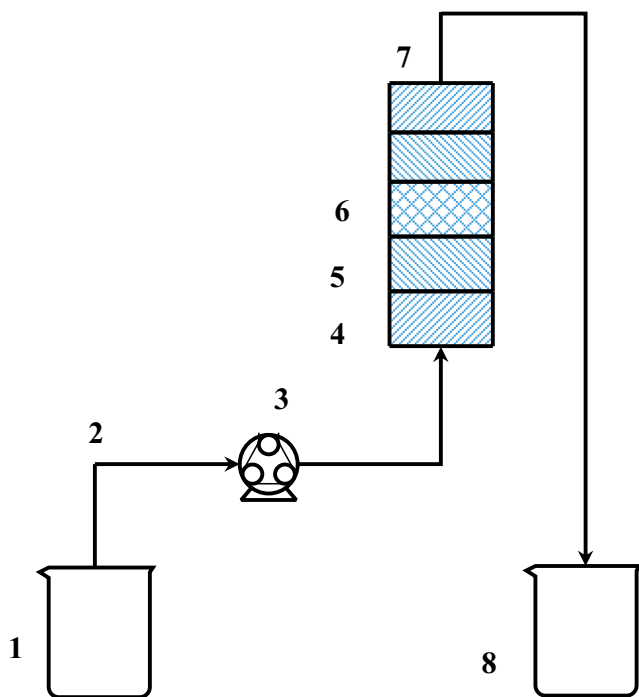
Fig. 1 Schematic diagram of fixed bed column 1. Synthetic solution of Cr(VI); 2. Silicon tube; 3. Peristaltic pump; 4. Glass beads; 5. Glass wool; 6. Adsorbent bed (activated carbon); 7. Column; 8. Effluents

the influence of variable functions like adsorbent's bed height (1, 2, and 3 cm), sorbate solution flow rate (2, 4, and 6 mL/min), and initial Cr(VI) species concentration (50, 100, and 150 mg/L). To study the effect of such variable parameters, experiments were carried out by keeping two parameters constant and one variable at a time. The effluent sample was collected at periodic intervals from the outlet and was then analyzed by a UV–visible spectrophotometer (Shimadzu, Japan) at 540 nm. Column studies were continued until the effluent Cr(VI) ion concentration at time t (C_t) equals the influent Cr(VI) ion concentration C_0.

Analysis and modeling of column data

The performance of fixed bed column in sequestering Cr(VI) species was analyzed by studying the breakthrough curves; a concentration–time profile curve represented as the ratio of metal species concentration of effluent solution to the metal species concentration of influent solution against column run time under a given set of conditions. In addition, the shape and appearance of breakthrough curve can be defined as function of breakthrough points and exhaustion time of the column run. The breakthrough point (t_b) represents the time when the permissible limit of metal concentration is 0.05 times that of metal in the effluent solution, i.e., $C_t = 0.05C_0$. The exhaustion time in column can be calculated in terms of time where effluent concentration reaches approximately equal to the influent concentration ($C_t = 0.95C_0$). The maximum metal loading

of column could be obtained by measuring the area (A) above the breakthrough curve at a given condition (Hasan et al. 2010). Total effective volume of effluent which passes through the column for treating Cr(VI) species can be represented as:

$$V_{eff} = Qt_{total} \tag{1}$$

Here, t_{total} and Q represent the exhaustion point in terms of time and the flow rate (mL/min), respectively. Moreover, breakthrough curve represents the behavior of metal species loading on packed bed of column in relation to adsorbed concentration (C_{ads} = influent concentration (C_0) − effluent concentration (C_t)). The total adsorbed chromium concentration (q_{total} in mg) in the column can be estimated by integrating the adsorbed metal concentration at a given condition as per the following equation (Luo et al. 2011; Talat et al. 2018).

$$q_{total} = \frac{QA}{1000} = \frac{Q}{1000}\int_{t_0}^{t_{total}} C_{ad}\, dt = \frac{Q}{1000}\int_{t_0}^{t_{total}} (C_0 - C_t)\, dt \tag{2}$$

The total Cr(VI) species (m_{total}) processed through the packed bed column can be estimated by the following equation (Luo et al. 2011; Talat et al. 2018) (3)

$$m_{total} = \frac{C_0 Q t_{total}}{1000} \tag{3}$$

Removal efficiency (%) of Cr(VI) species with respect to the flowing volume could be analyzed from the ratio of Cr(VI) species adsorbed (q_{total}) to the quantity of Cr(VI) species processed (m_{total}) through the column. The equation is represented as follows (Luo et al. 2011; Talat et al. 2018):

$$Y(\%) = \frac{q_{total}}{m_{total}} \times 100 \tag{4}$$

The maximum adsorption capacity or the equilibrium uptake capacity ($q_{e(exp)}$) per unit of the adsorbent in the fixed packed bed column can be assessed by the expression (Talat et al. 2018)

$$q_{e(exp)} = \frac{q_{total}}{X} \tag{5}$$

Results and discussion

Characteristic analysis of adsorbent

Surface area and CHNS analysis

In order to evaluate the adsorptive capability of an adsorbent, surface area and functional groups of adsorbent's surface play an important role. The BET total pore analysis revealed that BET surface area and t-Plot micropore volume are 782.89 m²/g and 0.134 cm³/g,

respectively. In addition, the BJH adsorption and desorption average pore diameter are 3.26 nm and 3.15 nm, respectively, which signifies that the adsorbent is mesoporous in nature. The percentage of C, H, N, and S of derived adsorbent are 46.14%, 6.69%, 3.09%, and 0%, respectively.

FESEM and EDAX analysis

The examination of the morphological properties of the adsorbent was performed by FESEM. Figure 2a and b elucidates the micrograph of adsorbent prior and after uptake of Cr(VI) species. Prior to adsorption, the adsorbent surface has rough and


Fig. 2 SEM micrographs: (**a**) before adsorption and (**b**) after Cr (VI) loaded on PWCS
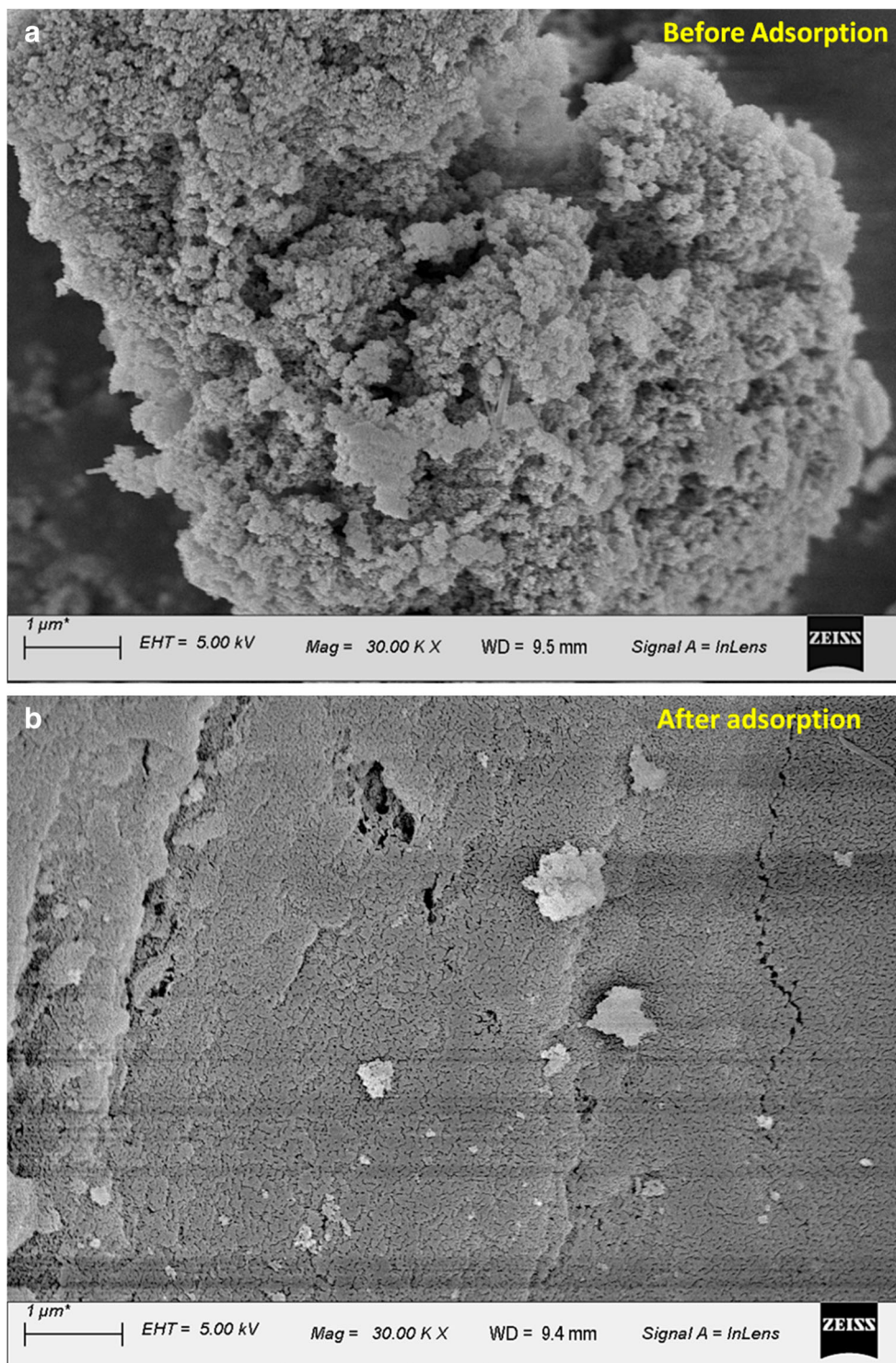
porous surface morphology due to the presence of pores and cavities as shown in Fig. 2a. It is attributed to the release of volatile gases from the inner surface of biomass during its thermal decomposition which leads to rougher and porous surface of adsorbent. At the same time, after the Cr(VI) adsorption, these cavities tend to fill and thus the surface turns into smooth surface morphology as shown in Fig. 2b, and this

result can also be supported by FTIR and EDX analysis. EDX spectral analysis is used to describe the qualitative elemental constitution. As shown in Fig. 3b, EDX revealed the presence of Cr(VI) species after the adsorption; however, no such characteristic peak of Cr(VI) was obtained before the adsorptions shown in Fig. 3a. Similar analysis and reasoning were reported by Majumder et al. (2017).

Fig. 3 (a) The EDS of PWC shell before adsorption. (b) EDS spectra of PWC shell after adsorption
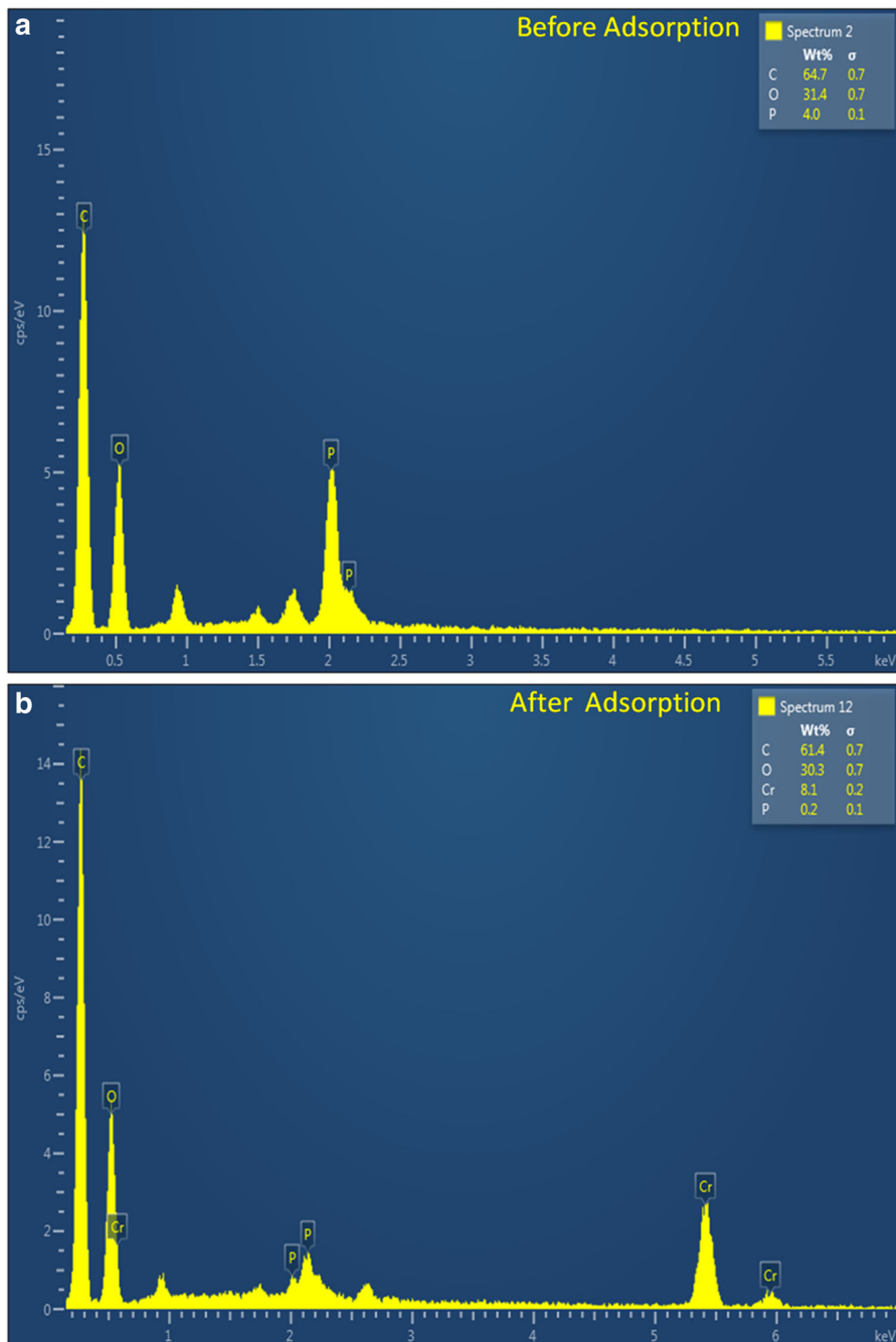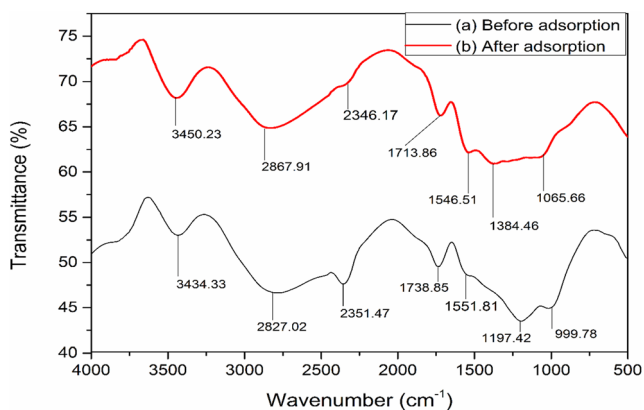
Fig. 4 The FTIR spectra of PWC shell before and after adsorption of Cr(VI)

FTIR spectral analysis

FTIR spectral analysis allows us to understand the interaction behavior of different functional groups on the adsorbent with metal ion. In order to observe the result, the biomass was complexed with KBr powder in the ratio of 1:100 (weight by weight) and spectral analysis were verified in the range of 4000–500 cm^{-1}. FTIR spectra of PWCS (activated adsorbent) prior and after the loading of Cr(VI) species show the complex nature of adsorbent as shown in Fig. 4a and b. The band peaks at 3450.23, 2867.91, 2346.91, 1713.86, 1546.51, 1384.46, and 1065.66 were assigned to O–H stretching, aliphatic C–H stretching, nitrile C≡N stretch, the C=O stretching, amide C–O stretching, carboxylate anion C=O stretching, and CO of alcohols and carboxylic acids (Singha et al. 2011), respectively. As shown in FTIR spectra (Fig. 4 b), the adsorption peak intensities of adsorbent after loading the Cr(VI) either decreased or shifted. For example, the adsorption peaks at 3450.23, 2867.91, 2346.91, 1713.86, 1546.51, 1384.46, and 1065.66 were shifted to 3434.33, 2827.02, 2351.47, 1738.85, 1551.81, 1197.42, and 999.78 cm^{-1}, respectively, indicating the involvement of these functional groups in binding of Cr(VI) ion on adsorbent.
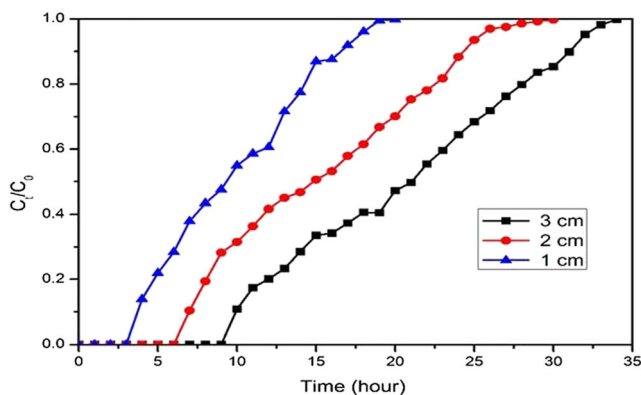
Fig. 5 Breakthrough curves of Cr(VI) removal by PWC shell for different bed depths

Influence of column bed height

Adsorption of Cr(VI) ions in packed bed column was examined by altering the adsorbent's bed height in the column from 1 to 3 cm at initial sorbate concentration of 50 mg/L and at constant column flow rate of 2 mL/min. Moreover, 1, 2, and 3 g of PWCS powder were added to yield adsorbent column bed heights of 1, 2, and 3 cm, respectively. As elucidated in Fig. 5, elevated breakthrough time and exhaustion time were achieved with elevated adsorbent's column bed height. Furthermore, the adsorption capacity, volume treated, and percent removal on PWCS adsorbent for Cr(VI) removal increased with increased adsorbent's bed height, and the results are shown in Table 1. It may be because the increase in contact time of adsorbate with adsorbent due to increase in bed height allows more diffusion of Cr(VI) species into PWCS. However, increased bed height resulted in higher surface area which in turn provided more availability of active site on adsorbent surface for adsorption of Cr(VI) species. Similar analysis and reasoning were reported by Yüksel and Orhan (2019).

Influence of sorbate flow rate

Efficient adsorptive performance of the packed bed column was significantly affected by sorbate flow rate. The sorbate's flow rate in the column was altered from 2 to 6 mL/min with an initial Cr(VI) ion concentration of 50 mg/L and with 2 cm of adsorbent's column bed height. Column breakthrough curve was achieved by plotting the C_t/C_0 versus time as depicted in Fig. 6. Here, C_0 and C_t represent the Cr(VI) species concentration in the influent and effluent, respectively. Figure 6 verifies the breakthrough time (t_b) and exhaustion point (t_e) of time have depreciated with elevated flow rates of influent. In addition, as flow rates of the influent elevated from 2.0 to 6.0 mL/min, this resulted in decreased Cr(VI) species removal efficiency from 51.06% to 48.59% as shown in Table 1. This attributes to the decreased sorbate–sorbent contact time and lowered external film mass resistance with increased influent rate. As a result, Cr(VI) species leaving the adsorbent without being adsorbed in column from the effluent resulted in decreased saturation time. Similar consistency has been reported by other researches also like Banerjee et al. (2017), Jain et al. (2013), and Rangabhashiyam et al. (2016).

Influence of inlet Cr(VI) species concentration

To study the influence of initial sorbate concentration, the Cr(VI) species concentration was altered from 50 to 150 mg/L while other variables were held constant such as sorbate flow rate of 2 mL/min and sorbent's column bed height of 2 cm. As depicted in Fig. 7, the fixed bed exhaustion time (t_e) and breakthrough time (t_b) depreciated from 29 to 19 h and 7 to 2 h, respectively, with elevating sorbate concentration
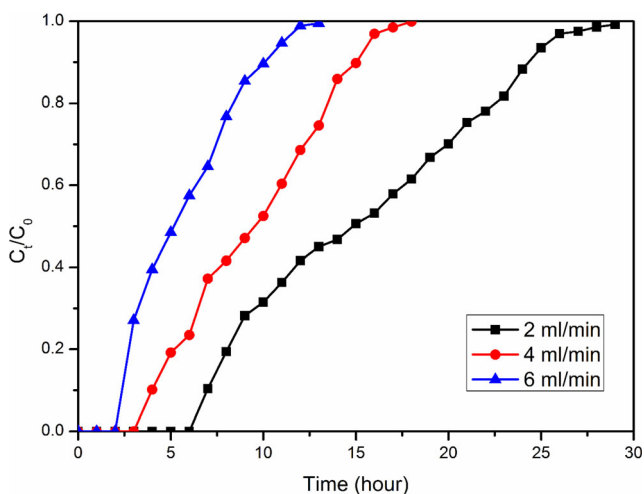
Table 1 Column data analysis at various operating parameters for Cr(VI) adsorption using PWC shell

Z (cm)	Q (L/h)	C_0 (mg/L)	t_{total} (h)	m_{total} (mg)	q_{total} (mg)	$q_{e(exp)}$ (mg/g)	V_{eff} (mL)	Y (%)
1	0.12	50	21	126	64.33	64.33	2.52	51.06
2	0.12	50	29	174	91.27	45.63	3.48	52.46
3	0.12	50	35	216	122.63	40.87	4.32	56.78
2	0.24	50	18	216	113.29	56.64	4.32	52.45
2	0.36	50	13	234	102.00	51.00	4.68	43.59
2	0.12	100	23	276	127.80	63.90	2.76	46.30
2	0.12	150	19	342	140.40	70.20	2.28	41.05

from 50 to 150 mg/L. This could possibly be due to quicker saturation of sorbate binding sites of PWCS at elevated sorbate concentration, hence breakthrough curve becomes steeper. As reported in Table 1, the Cr(VI) species removal efficiency reduced with elevated initial Cr(VI) species concentration. This may be due to the additional amount of solute entering in the column at high concentration while less amount was adsorbed on the adsorbent. The adsorption capacity of the column elevated with increased sorbent influent concentration. This could be due to concentration gradient of the Cr(VI) metal ion in the sorbate solution and on the adsorbent. Thus, higher inlet concentration causes more driving force which is responsible for elevated diffusion coefficients or mass transfer coefficients and hence adsorption capacity increased. Similar investigations have been carried out by Radnia (2013), Jain et al. (2013), and Banerjee et al. (2017).

Modeling of the packed bed column breakthrough curves

Breakthrough curves and dynamic behavior of column was investigated at given conditions like sorbate column flow rate, initial Cr(VI) species concentration, and adsorbent column bed height. Adsorption data thus obtained from the column study was analyzed by several column models like Adams–Bohart model, Thomas model, Yoon–Nelson model, and BDST model. The laboratory-scale result tested by these models could be used for industrial-grade fixed bed column design.

Thomas model

This model has been widely employed to define the performance of the packed bed column and it follows the Langmuir assumption adsorption process without axial dispersion. It explains about the adsorption process which adheres to reversible second-order kinetics and the linear form of the equation can be represented as (Baral et al. 2009)

$$\ln\left(\frac{C_0}{C_t}-1\right) = \frac{K_{TH}q_0W}{Q} - K_{TH}C_0t \qquad (6)$$

Here, K_{TH} (mL/min mg) and q_0 (mg/g) represent the Thomas model constant and the adsorption capacity of adsorbent, respectively; W (g) is weight of sorbent in the fixed bed column; Q (mL/min) indicates the flow rate of sorbate in column; and C_0/C_t denotes the ratio of influent to effluent concentration of metal solution. The unknown

Fig. 6 Breakthrough curves of Cr(VI) removal by PWC shell for different flow rates
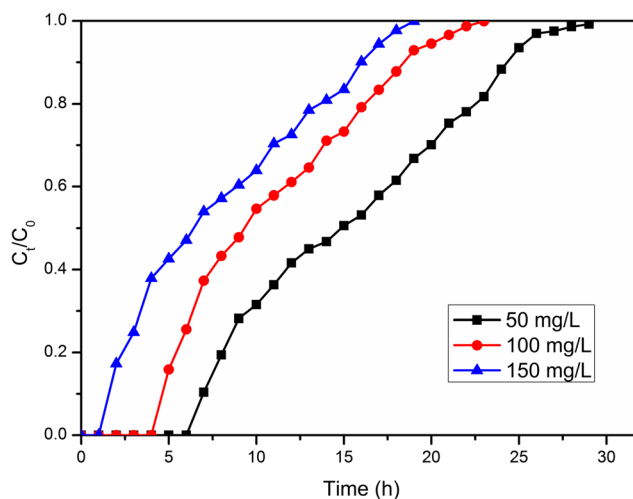
Fig. 7 Breakthrough curves of Cr(VI) removal by PWC shell for different initial Cr(VI) concentrations

Table 2 Parameters of various models for Cr(VI) adsorption by PWC shell in packed bed adsorption at various conditions

Experimental conditions			Thomas model			Adams–Bohart model			Yoon–Nelson model		
Z (cm)	Q (L/H)	C_0 (mg/L)	q_0 (mg/g)	K_{TH} (L/H mg)	R^2	N_{AB} (mg/L)	K_{AB} (L/mg h)	R^2	K_{YN} (1/h)	τ (h)	R^2
1	0.12	50	55.44	0.008	0.890	8340.88	0.0021	0.880	0.407	9.241	0.890
2	0.12	50	87.31	0.005	0.930	6141.86	0.0016	0.854	0.262	14.552	0.930
3	0.12	50	117.36	0.005	0.876	5042.04	0.0015	0.920	0.238	19.560	0.876
2	4	50	107.92	0.010	0.880	7524.31	0.0028	0.875	0.503	8.993	0.880
2	6	50	96.17	0.012	0.945	8178.71	0.0024	0.892	0.589	5.343	0.945
2	2	100	121.68	0.003	0.866	9578.00	0.0008	0.829	0.338	10.140	0.866
2	2	150	129.02	0.002	0.801	11,993.78	0.0006	0.855	0.329	7.168	0.801

values of K_{TH} and q_0 of Thomas equation was determined by slope and intercept, respectively, of linear plot for ln $((C_0/C_t) - 1)$ versus t using linear regression form (figures not shown) and results are tabulated in Table 2. Regression values (R^2) of this model range from 0.801 to 0.945 suggesting the best fit as compared to other models. Table 2 also denotes that as adsorbent's bed height of the column increased, q_0 values also elevated with reduction of K_{TH} values. Elevation in Cr(VI) initial concentration resorted to increased q_0 values while reducing K_{TH} values. Adsorption driving force refers to difference of sorbate concentration on the adsorbent (PWCS) and in the solution. In addition, an elevated volumetric flow rate resulted in decreased q_0 values with increased K_{TH}. This possibly could be due to less residence time between the Cr(VI) ions and adsorbent in the packed column bed. Similar trends were reported by other researchers like Chen et al. (2012), Zang et al. (2017), and Baral et al. (2009).

Adams–Bohart model

Adams–Bohart model uses surface reaction theory to define the fundamental equations. It explains the initial breakthrough curve C_t/C_0 against t values of the fixed bed column. This approach is based on some assumptions like equilibrium does not occur suddenly and the extent of adsorption is proportionally related to the extent of vacant active sites left over the adsorbent's surface (Goel et al. 2005; Sharma and Singh 2013). The ability of the adsorbent in adsorbing the sorbate molecules can be observed by the following equation:

$$\ln\left(\frac{C_t}{C_0}\right) = K_{AB} C_0\, t - K_{AB} N_{AB}\left(\frac{Z}{u}\right) \tag{7}$$

Here, C_t (mg/L) and C_0 (mg/L) represent the effluent and influent Cr(VI) species concentration, respectively; K_{AB} (L/mg/min) and N_{AB} (mg/L) indicate the kinetics

and saturation constant, respectively; Z (cm) represents the adsorbent's bed height in column and U (cm/min) denotes the superficial velocity that can be elucidated by dividing the column flow rate to the cross-sectional area of adsorbent bed. The $\ln\left(\frac{C_t}{C_0}\right)$ versus time was used to determine the unknown parameters, i.e., K_{AB} and N_{AB} using slope and intercept, respectively, and the data for the same has been tabulated in Table 2. As shown in Table 2, the elevated adsorbent's bed height of column as well as sorbate flow rate causes a decrease in value of N_{AB} and K_{AB}. In addition, elevated initial concentration of Cr(VI) species resulted in increased and decreased N_{AB} and K_{AB} values, respectively. Such results can be attributed to the external mass transfer in adsorption of Cr(VI) ions at initial part of the column. The determined linear regression values (R^2) ranged from between 0.880 and 0.920. Low values of R^2 suggest Bohart–Adams model is inappropriate in predicting the behavior of fixed bed column (Mahmoud 2016).
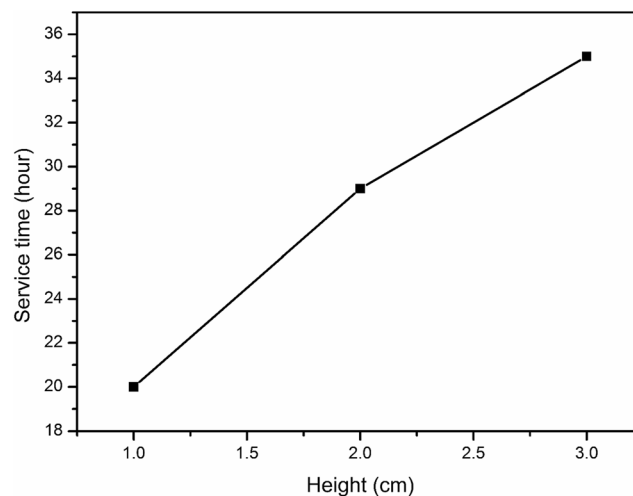
Fig. 8 Linear plots of bed depth service time model

Table 3 Bed depth service time (BDST) model

N_0 (mg/L)	K_a (L/mg h)	Slope	Intercept	R^2
3582.803	0.003313	7.5	13	0.9868

Yoon–Nelson model

Yoon–Nelson model assumes that the feasibility of reduced rate of sorption directly depends on the possibility of sorbate adsorption on the sorbent and the possibility of sorbate breakthrough on the sorbent surface (Chen et al. 2012). Yoon–Nelson model expression can be represented as

$$\ln\left(\frac{C_t}{C_0 - C_t}\right) = K_{YN}t - K_{YN}\,\tau \quad (8)$$

Here, K_{YN} (L/min) and τ (min) represent the rate constant and time to reach 50% sorbate breakthrough, respectively, and t represents the processing time. The two unknown parameters of Yoon–Nelson model, i.e., K_{YN} and τ, can be verified from the linear plot of $\ln(C_t/C_0 - C_t)$ versus time using its slope and intercept, respectively, and the calculated data are as represented in Table 2. Table 2 verifies that the time needed to reach 50% breakthrough (τ) is elevated and the rate constant K_{YN} is reduced with the elevation of the adsorbent's bed height column. An increase in sorbate flow rate resulted in increased rate constant K_{YN} and decreased τ values. These results attribute to quick saturation of packed bed column and less residence time of the Cr(VI) species in the adsorbent bed. Regression values (R^2) from Table 2 suggest the applicability of Thomas and Yoon–Nelson models for adsorption of Cr(VI) species in the fixed bed column. Similar analysis and reasoning were reported by other authors (Chen et al. 2012; Ahmad and Hameed 2010).

Bed depth service time (BDST) model

This model was studied to extend the laboratory-scale design for pilot-scale application to presume the behavior of fixed bed column. BDST model explains the physical adsorption without considering the external mass resistance and intraparticle mass transfer resistance (Vimala et al. 2011; Vinodhini and Das 2010). BDST described the relationship between the processing time (t) and column bed height (Z). BDST model equation can be represented as follows:

$$t = \left(\frac{N_0 Z}{C_0 u}\right) - \left(\frac{1}{C_0 K_a}\right)\ln\left(\frac{C_0}{C_b} - 1\right) \quad (9)$$

Here, C_b and C_0 represent the breakthrough metal concentration and influent concentration, respectively, u represents the linear velocity (cm/min), K_a indicates the column rate constant (L/mg min), and N_0 represents the adsorption capacity (mg/L). The plot for service time versus bed height gave a straight line at the sorbate flow rate of 2 mL/min and the same has been represented in Fig. 8. Regression values ($R^2 = 1$) were calculated using linear regression, and it suggests the better fitting of BDST model for fixed bed column. Rate constant (K_a) and sorption capacity (N_0) were calculated using the intercept and slope from the straight-line equation of BDST model and data thus calculated are represented in Table 3. The observed values of K_a and N_0 were observed to be 0.043071 and 1433.121, respectively. Notably, if K_a values are large, a short column bed height will avoid the breakthrough while decreasing K_a values suggest the requirement of longer bed heights to avoid the breakthrough (Hasan et al. 2010). BDST model parameters can be implemented for further pilot-scale trials.

Conclusion

The present investigation verifies the activated carbon derived from acid-activated *T. natans* shell (PWCS) waste as a adsorbent for efficiently removing Cr(VI) species from simulated solutions using fixed bed column. Influence of sorbate initial concentration, adsorbent's column bed height, and sorbate flow rate on breakthrough curves were studied for fixed bed column. A low initial metal ion concentration, a higher bed height, and a lower flow rate cause higher exhaustion time and breakthrough point. Adsorption efficiency (%) of Cr(VI) species elevated with rising bed height and it reduced with elevated influent Cr(VI) species and sorbent inlet flow rate. The experimental result revealed that percentage removal for Cr(VI) from aqueous solution having pH 2 and temperature 303.15 K was observed to be 52.46% at 2 cm height, 50 mg/L influent concentration, and 1.2 L/h flow rate. The maximum adsorption capacity was estimated to be 87.31 mg/g according to the Thomas model. Several mathematical models such as the Adams–Bohart, Thomas, Yoon–Nelson, and BDST model were used to verify the experimental data of fixed bed column. Performance of breakthrough curve was better explained by Thomas model due to its good correlation coefficient R^2 (0.801–0.945) than other models. The BDST model was successfully able to assume the parameters for design of pilot-scale plant and observed K_a (L/mg h) value and R^2 was 0.003 and 0.98, respectively. The study revealed that acid-treated *T. natans* shell proved a potent alternative for adsorbent in fixed bed column for the removal of Cr(VI) species from simulated wastewater.

References

Ahmad AA, Hameed BH (2010) Fixed-bed adsorption of reactive azo dye onto granular activated carbon prepared from waste. J Hazard Mater 175:298–303. https://doi.org/10.1016/j.jhazmat.2009.10.003

Almeida JC, Cardoso CED, Tavares DS, Freitas R, Trindade T, Vale C, Pereira E (2019) Chromium removal from contaminated waters using nanomaterials—a review. TrAC Trends Anal Chem 118: 277–291. https://doi.org/10.1016/j.trac.2019.05.005

Banerjee M, Bar N, Basu RK, Das SK (2017) Comparative study of adsorptive removal of Cr(VI) ion from aqueous solution in fixed bed column by peanut shell and almond shell using empirical models and ANN. Environ Sci Pollut Res Int 24:10604–10620. https://doi.org/10.1007/s11356-017-8582-8

Barakat MA (2011) New trends in removing heavy metals from industrial wastewater. Arab J Chem 4:361–377. https://doi.org/10.1016/j.arabjc.2010.07.019

Baral SS, Das N, Ramulu TS, Sahoo SK, Das SN, Chaudhury GR (2009) Removal of Cr(VI) by thermally activated weed Salvinia cucullata in a fixed-bed column. J Hazard Mater 161:1427–1435. https://doi.org/10.1016/j.jhazmat.2008.04.127

Bishnoi NR, Bajaj M, Sharma N, Gupta A (2004) Adsorption of Cr(VI) on activated rice husk carbon and activated alumina. Bioresour Technol 91:305–307. https://doi.org/10.1016/S0960-8524(03)00204-9

Chen S, Yue Q, Gao B, Li Q, Xu X, Fu K (2012) Adsorption of hexavalent chromium from aqueous solution by modified corn stalk: a fixed-bed column study. Bioresour. Technol. 113:114–120. https://doi.org/10.1016/j.biortech.2011.11.110

Cherdchoo W, Nithettham S, Charoenpanich J (2019) Removal of Cr(VI) from synthetic wastewater by adsorption onto coffee ground and mixed waste tea. Chemosphere 221:758–767. https://doi.org/10.1016/j.chemosphere.2019.01.100

Demirbas E, Kobya M, Senturk E, Ozkan T (2004) Adsorption kinetics for the removal of chromium (VI) from aqueous solutions on the activated carbons prepared from agricultural wastes. Water SA 30: 533–539

Dubey SP, Gopal K (2007) Adsorption of chromium(VI) on low cost adsorbents derived from agricultural waste material: a comparative study. J Hazard Mater 145:465–470. https://doi.org/10.1016/j.jhazmat.2006.11.041

El-Sherif IY, Tolani S, Ofosu K, Mohamed OA, Wanekaya AK (2013) Polymeric nanofibers for the removal of Cr(III) from tannery waste water. J Environ Manag 129:410–413. https://doi.org/10.1016/j.jenvman.2013.08.004

EPA (1990) Environmental Pollution Control Alternatives. EPA/625/5-90/025, EPA/625/4-89/023, Cincinnati (accessed on 11/09/2019)

Goel J, Kadirvelu K, Rajagopal C, Kumar VG (2005) Removal of lead(II) by adsorption using treated granular activated carbon: batch and column studies. J Hazard Mater 125:211–220. https://doi.org/10.1016/j.jhazmat.2005.05.032

Hasan SH, Ranjan D, Talat M (2010) Agro-industrial waste "wheat bran" for the biosorptive remediation of selenium through continuous up-flow fixed-bed column. J Hazard Mater 181:1134–1142. https://doi.org/10.1016/j.jhazmat.2010.05.133

Jain M, Garg VK, Kadirvelu K (2013) Cadmium(II) sorption and desorption in a fixed bed column using sunflower waste carbon calcium–alginate beads. Bioresour Technol 129:242–248. https://doi.org/10.1016/j.biortech.2012.11.036

Kan C-C, Ibe AH, Rivera KKP, Arazo RO, de Luna MDG (2017) Hexavalent chromium removal from aqueous solution by adsorbents synthesized from groundwater treatment residuals. Sustain Environ Res 27:163–171. https://doi.org/10.1016/j.serj.2017.04.001

Kelly-Vargas K, Cerro-Lopez M, Reyna-Tellez S, Bandala ER, Sanchez-Salas JL (2012) Adsorption of heavy metals in polluted water, using

different waste fruit cortex. Phys. Chem. Earth, Parts A/B/C. 37–39: 26–29. https://doi.org/10.1016/j.pce.2011.03.006

Kumar S, Selvaraju N, Prasanna VR (2018) Removal of Cr(VI) from synthetic solutions using water caltrop shell as a low-cost biosorbent. Sep Sci Technol 54:2783–2799. https://doi.org/10.1080/01496395.2018.1560333

Luo X, Deng Z, Lin X, Zhang C (2011) Fixed-bed column study for Cu2+ removal from solution using expanding rice husk. J Hazard Mater 187:182–189. https://doi.org/10.1016/j.jhazmat.2011.01.019

Lyu H, Tang J, Huang Y, Gai L, Zeng EY, Liber K, Gong Y (2017) Removal of hexavalent chromium from aqueous solutions by a novel biochar supported nanoscale iron sulfide composite. Chem Eng J 322:516–524. https://doi.org/10.1016/j.cej.2017.04.058

Ma H, Yang J, Gao X, Liu Z, Liu X, Xu Z (2019) Removal of chromium (VI) from water by porous carbon derived from corn straw: influencing factors, regeneration and mechanism. J Hazard Mater 369:550–560. https://doi.org/10.1016/j.jhazmat.2019.02.063

Mahmoud MA (2016) Kinetics studies of uranium sorption by powdered corn cob in batch and fixed bed system. J Adv Res 7:79–87. https://doi.org/10.1016/j.jare.2015.02.004

Majumder R, Sheikh L, Naskar A, Vineeta, Mukherjee M, Tripathy S (2017) Depletion of Cr(VI) from aqueous solution by heat dried biomass of a newly isolated fungus Arthrinium malaysianum: a mechanistic approach. Sci Rep 7:1–15. https://doi.org/10.1038/s41598-017-10160-0

Mohanty K, Jha M, Meikap BC, Biswas MN (2005) Removal of chromium (VI) from dilute aqueous solutions by activated carbon developed from Terminalia arjuna nuts activated with zinc chloride. Chem Eng Sci 60:3049–3059. https://doi.org/10.1016/j.ces.2004.12.049

Owalude SO, Tella AC (2016) Removal of hexavalent chromium from aqueous solutions by adsorption on modified groundnut hull. Beni-Suef Univ J Basic Appl Sci 5:377–388. https://doi.org/10.1016/j.bjbas.2016.11.005

Patra C, Medisetti RMN, Pakshirajan K, Narayanasamy S (2019) Assessment of raw, acid-modified and chelated biomass for sequestration of hexavalent chromium from aqueous solution using Sterculia villosa Roxb. shells. Environ Sci Pollut Res 26(23): 23625–23637. https://doi.org/10.1007/s11356-019-05582-4

Pillai MG, Simha P, Gugalia A (2014) Recovering urea from human urine by bio-sorption onto microwave activated carbonized coconut shells: equilibrium, kinetics, optimization and field studies. J Environ Chem Eng 2:46–55. https://doi.org/10.1016/j.jece.2013.11.027

Radnia H (2013) Adsorption of Fe(II) from aqueous phase by chitosan: application of physical models and artificial neural network for prediction of breakthrough. Int J Eng 26. https://doi.org/10.5829/idosi.ije.2013.26.08b.06

Rai MK, Shahi G, Meena V, Meena R, Chakraborty S, Singh RS, Rai BN (2016) Removal of hexavalent chromium Cr (VI) using activated carbon prepared from mango kernel activated with H3PO4. Resour.-Effic. Technol. 2:S63–S70. https://doi.org/10.1016/j.reffit.2016.11.011

Rai PK, Lee SS, Zhang M, Tsang YF, Kim K-H (2019) Heavy metals in food crops: health risks, fate, mechanisms, and management. Environ Int 125:365–385. https://doi.org/10.1016/j.envint.2019.01.067

Rangabhashiyam S, Nandagopal MS, Nakkeeran E, Selvaraju N (2016) Adsorption of hexavalent chromium from synthetic and electroplating effluent on chemically modified Swietenia mahagoni shell in a packed bed column. Environ Monit Assess 188:411–411. https://doi.org/10.1007/s10661-016-5415-z

Sharma R, Singh B (2013) Removal of Ni (II) ions from aqueous solutions using modified rice straw in a fixed bed column. Bioresour Technol 146:519–524. https://doi.org/10.1016/j.biortech.2013.07.146

Singha B, Naiya TK, Bhattacharya AK, Das SK (2011) Cr(VI) ions removal from aqueous solutions using natural adsorbents—FTIR studies. J Environ Prot 2:729–735. https://doi.org/10.4236/jep.2011.26084

Talat M, Mohan S, Dixit V, Singh DK, Hasan SH, Srivastava ON (2018) Effective removal of fluoride from water by coconut husk activated carbon in fixed bed column: experimental and breakthrough curves analysis. Groundw Sustain Dev 7:48–55. https://doi.org/10.1016/j.gsd.2018.03.001

Vimala R, Charumathi D, Das N (2011) Packed bed column studies on cd(II) removal from industrial wastewater by macrofungus Pleurotus platypus. Desalination 275:291–296. https://doi.org/10.1016/j.desal.2011.03.014

Vinodhini V, Das N (2010) Packed bed column studies on Cr (VI) removal from tannery wastewater by neem sawdust. Desalination 264:9–14. https://doi.org/10.1016/j.desal.2010.06.073

World Health Organization (2004) Guidelines for Drinking-Water Quality, third ed. World Health Organization, Geneva ISBN 92 4 154638 7

Yu J, Jiang C, Guan Q, Ning P, Gu J, Chen Q, Zhang J, Miao R (2018) Enhanced removal of Cr(VI) from aqueous solution by supported ZnO nanoparticles on biochar derived from waste water hyacinth. Chemosphere 195:632–640. https://doi.org/10.1016/j.chemosphere.2017.12.128

Yüksel Ş, Orhan R (2019) The removal of Cr(VI) from aqueous solution by activated carbon prepared from apricot, peach stone and almond shell mixture in a fixed-bed column. Arab J Sci Eng 44:5345–5357. https://doi.org/10.1007/s13369-018-3618-z

Zang T, Cheng Z, Lu L, Jin Y, Xu X, Ding W, Qu J (2017) Removal of Cr(VI) by modified and immobilized Auricularia auricula spent substrate in a fixed-bed column. Ecol Eng 99:358–365. https://doi.org/10.1016/j.ecoleng.2016.11.070

Zhang X, Lv L, Qin Y, Xu M, Jia X, Chen Z (2018) Removal of aqueous Cr(VI) by a magnetic biochar derived from Melia azedarach wood. Bioresour Technol 256:1–10. https://doi.org/10.1016/j.biortech.2018.01.145